Journal of Computational Physics 229 (2010) 1198–1212

Contents lists available at ScienceDirect

Journal of Computational Physics

journal homepage: www.elsevier.com/locate/jcp

Schur-decomposition for 3D matrix equations and its application in solving radiative discrete ordinates equations discretized by Chebyshev collocation spectral method

Ben-Wen Li *, Shuai Tian, Ya-Song Sun, Zhang-Mao Hu

Key Laboratory of Electromagnetic Processing of Materials (Ministry of Education), Northeastern University, P.O. Box 314, Shenyang, Liaoning 110004, China

ARTICLE INFO

Article history:
Received 17 June 2009
Received in revised form 4 October 2009
Accepted 13 October 2009
Available online 28 October 2009

Keywords:
Schur-decomposition
Matrix-diagonalization
Tensor product
Spectral methods
Radiative transfer equation
Discrete ordinates method

ABSTRACT

The Schur-decomposition for three-dimensional matrix equations is developed and used to directly solve the radiative discrete ordinates equations which are discretized by Chebyshev collocation spectral method. Three methods, say, the spectral methods based on 2D and 3D matrix equation solvers individually, and the standard discrete ordinates method, are presented. The numerical results show the good accuracy of spectral method based on direct solvers. The CPU time cost comparisons against the resolutions between these three methods are made using MATLAB and FORTRAN 95 computer languages separately. The results show that the CPU time cost of Chebyshev collocation spectral method with 3D Schur-decomposition solver is the least, and almost only one thirtieth to one fiftieth CPU time is needed when using the spectral method with 3D Schur-decomposition solver compared with the standard discrete ordinates method.

1. Introduction

The robust and efficient solving of the matrix equation

$$AX + XB = C \tag{1}$$

plays a very important role in the numerical computation of many fields such as control theory [1], stability of linear system [2], computational fluid dynamics (CFD) [3–6], etc. Eq. (1) is so called Sylvester equation. The matrices A, B and C in Eq. (1) are all real, and $A \in R^{m\times m}, B \in R^{n\times n}, C \in R^{m\times n}$. It is well know that Eq. (1) has a unique solution if and only if the eigenvalues $\varepsilon_1, \varepsilon_2, \ldots, \varepsilon_m$ of A and $\rho_1, \rho_2, \ldots, \rho_n$ of B satisfy $\varepsilon_i + \rho_j \neq 0$ $(i = 1, 2, \ldots, m;\ j = 1, 2, \ldots, n)$. According to the eigenvalue properties of matrices A and B, different algorithms were proposed for Eq. (1). For example, the matrix-diagonalization procedure [3–7] is direct and very efficient when the eigenvalues of A and B are real. However, when the eigenvalues of A and B are complex, the Schur-decomposition (Hesenberg–Schur or Schur-reduction are called also) [1,8] is also direct and very efficient, and further is used to avoid complex number computations. Another direct way for Eq. (1) is the tensor product method [9] in which the huge memory is needed special when large grid number is used. Some efficient iterative methods [2,10] for Eq. (1) under some special conditions are available. Unfortunately, the iterative methods are less and less employed in favor of the direct ones.

In general, the eigenvalue properties of coefficient matrices A and B in Eq. (1) are determined by numerical methods and physical problems. For example, when the Chebyshev collocation spectral method is adopted for steady-state advection-dif-

* Corresponding author. Tel.: +86 24 83681756; fax: +86 24 83681758.
E-mail addresses: heatli@hotmail.com, heatli@epm.neu.edu.cn (B.-W. Li).

0021-9991/$ - see front matter © 2009 Elsevier Inc. All rights reserved.
doi:10.1016/j.jcp.2009.10.025

fusion equation in fluid dynamics, the resultant algebraic system from the discretization of governing equation always has complex eigenvalues [11]. Under these kinds of situations, the Schur-decomposition should be the best choice for solving. While in numerical simulation of incompressible viscous flow, the Poisson equations appear after divergence free of Navier–Stokes equations, and the algebraic system from Chebyshev collocation spectral approximation has real eigenvalues. This time the matrix-diagonalization procedure is usually the most adapted [7].

In the area of thermal radiation, the three-dimensional radiative transfer equation (RTE), which takes the radiative intensity as unknown variable, is an advection-type partial differential equation (PDE), and only the first derivatives are included [12]. After discretization of RTE using Chebyshev collocation spectral method in space, the resultant algebraic system is a set of 3D matrix equations, and the eigenvalues of the coefficient matrices are complex. To the best knowledge of authors, there is not Schur-decompostion method for 3D matrix equations in references up to now.

In the reminder of this paper, the physical problem and its governing equation together with boundary condition will be presented in Section 2, the Chebyshev collocation spectral method is adopted to solve this problem numerically, and the resultant 3D matrix equations are formulated. The detailed Shur-decomposition method to solve the 3D matrix equations are described in Section 3. The results to show the superiorities of Schur-decomposition for 3D matrix equations and discussions are illustrated in Section 4. Finally, Section 5 gives the conclusions.

2. Physical problem and the Chebyshev matrix equations for discrete ordinates RTEs

2.1. Physical problem

Due to the high accuracy (exponential convergence or spectral accuracy) of spectral methods [13,14], the Chebyshev collocation spectral method was employed to solve thermal radiation by Li and co-authors [15–19]. As an extension of our recent works [15–19], the Chebyshev collocation spectral method is adopted to solve the radiative heat transfer in a 3D box-shaped furnace with absorbing-emitting media [20]. There exist steep temperature gradients in the axial direction of the furnace. The temperature profiles can be calculated according to the detailed description in Ref. [20]. First, the angular dependence of the problem is discretized by discrete ordinates method (DOM) [21–24]. The discrete ordinates representation of RTE in rectangular system for absorbing-emitting gray medium is

$$\mu^m \frac{\partial I^m}{\partial x} + \eta^m \frac{\partial I^m}{\partial y} + \xi^m \frac{\partial I^m}{\partial z} + K_a I^m = K_a I_b \tag{2}$$

where $I^m (m = 1, 2, \ldots, M)$ is the total radiation intensity at position (x, y, z) and in the direction m, whose direction cosine is (μ^m, η^m, ξ^m); K_a is the absorption coefficient of the medium; and I_b is the total blackbody radiation intensity at the temperature of the medium. Eq. (2) and represents M uncoupled partial differential equations for the M intensities, $I^m (m = 1, 2, \ldots, M)$.

In our first step to develop the Chebyshev collocation spectral method for this problem, we focus on the direct solver for Eq. (2) and just consider the situation of black boundary. Assuming all the boundaries are black, then the boundary condition for Eq. (2) is

$$I_{bw} = \sigma T_w^4 / \pi \tag{3}$$

where I_{bw} is the blackbody radiation intensity at the temperature of the surface, T_w; σ is the Stefan–Boltzmann constant. The detail boundary conditions together with length scale and optical thickness are dimensionlessly listed in Table 1.

2.2. Chebyshev matrix equations for discrete ordinates RTEs

In order to clearly understand, the following definitions are given.

Table 1
Dimensionless data for three-dimensional rectangular furnace fed to computer codes.

Dimensions of the furnace	$\widetilde{L}_x = 1, \widetilde{L}_y = 1, \widetilde{L}_z = 6$
Optical thickness	$\tau_0 = 1/6$
Wall blackbody intensities	$(\widetilde{I}_{bw})_{side} = 0.0020$
	$(\widetilde{I}_{bw})_{burner} = 0.0574$
	$(\widetilde{I}_{bw})_{end} = 0.0167$
Gas temperature	$\widetilde{T}_i = 0.1775$
	$\widetilde{T}_e = 0.6222$
	$\widetilde{T}_{\max} = 1$
Position of the peak	$Z'_{\max} = 0.8$
Slope of gas temperature distribution at furnace exit	$d_e = -0.22$

Definition 1. If A is a $m \times n$ 2D matrix, X is a $n \times p \times q$ 3D matrix, we use the symbol "$\square_{(1)}$" to denote the computation

$$Y = A\square_{(1)}X \text{ when it satisfy } y_{i,j,k} = \sum_{t=1}^{n} a_{i,t}x_{t,j,k}, \quad (1 \leqslant i \leqslant m,\ 1 \leqslant j \leqslant p,\ 1 \leqslant k \leqslant q).$$

Definition 2. If B is a $p \times m$ 2D matrix, X is a $n \times p \times q$ 3D matrix, we use the symbol "$\square_{(2)}$" to denote the computation

$$Y = X\square_{(2)}B \text{ when it satisfy } y_{i,j,k} = \sum_{t=1}^{p} x_{i,t,k}b_{t,j}, \quad (1 \leqslant i \leqslant n,\ 1 \leqslant j \leqslant m,\ 1 \leqslant k \leqslant q).$$

Definition 3. If C is a $q \times m$ 2D matrix, X is a $n \times p \times q$ 3D matrix, we use the symbol "$\square_{(3)}$" to denote the computation

$$Y = X\square_{(3)}C \text{ when it satisfy } y_{i,j,k} = \sum_{t=1}^{q} x_{i,j,t}c_{t,k}, \quad (1 \leqslant i \leqslant n,\ 1 \leqslant j \leqslant p,\ 1 \leqslant k \leqslant m).$$

Now the space dependence of the problem is expressed by Chebyshev polynomial and discretized by spectral collocation method similar as in [15–19].

First, the mapping of arbitrary domain $\{\Omega : (x,y,z) \in [X_1,X_2] \times [Y_1,Y_2] \times [Z_1,Z_2]\}$ to standard computational cube domain $\{D : (\alpha,\beta,\gamma) \in [-1,1] \times [-1,1] \times [-1,1]\}$ is needed to fit the requirement of Chebyshev polynomial

$$\begin{cases} \alpha = \frac{2x-(X_2+X_1)}{(X_2-X_1)}, & x = \frac{\alpha(X_2-X_1)+(X_2+X_1)}{2} \\ \beta = \frac{2y-(Y_2+Y_1)}{(Y_2-Y_1)}, & y = \frac{\beta(Y_2-Y_1)+(Y_2+Y_1)}{2} \\ \gamma = \frac{2z-(Z_2+Z_1)}{(Z_2-Z_1)}, & z = \frac{\gamma(Z_2-Z_1)+(Z_2+Z_1)}{2} \end{cases} \tag{4}$$

After mapping, Eq. (2) becomes

$$\mu^m\left(\frac{2}{X_2-X_1}\right)\frac{\partial I^m}{\partial\alpha} + \eta^m\left(\frac{2}{Y_2-Y_1}\right)\frac{\partial I^m}{\partial\beta} + \xi^m\left(\frac{2}{Z_2-Z_1}\right)\frac{\partial I^m}{\partial\gamma} + K_a I^m = K_a I_b \tag{5}$$

The Gauss–Lobatto collocation points [11,13,14] are used for spatial discretization for all three coordinates

$$\begin{cases} \alpha_i = -\cos\frac{\pi i}{N_x}, & i = 0,1,\ldots,N_x \\ \beta_j = -\cos\frac{\pi j}{N_y}, & j = 0,1,\ldots,N_y \\ \gamma_k = -\cos\frac{\pi k}{N_z}, & k = 0,1,\ldots,N_z \end{cases} \tag{6}$$

where N_x, N_y, N_z are the resolutions (number of grid points) in three coordinates, respectively.

The Chebyshev approximation of radiative intensity reads

$$I^m_{N_x,N_y,N_z}(\alpha,\beta,\gamma) = \sum_{k=0}^{N_z}\sum_{j=0}^{N_y}\sum_{i=0}^{N_x}\widehat{I}^m_{i,j,k}T_i(\alpha)T_j(\beta)T_k(\gamma) \tag{7}$$

where the $T_i(\alpha), T_j(\beta), T_k(\gamma)$ are the first kind Chebyshev polynomials, and the coefficients $\widehat{I}^m_{i,j,k}(i = 0,1,\ldots,N_x; j = 0,1,\ldots,N_y; k = 0,1,\ldots,N_z)$ are determined by requiring $I^m_{N_x,N_y,N_z}(\alpha,\beta,\gamma)$ to coincide with $I^m(\alpha,\beta,\gamma)$ at the collocation points $(\alpha_i,\beta_j,\gamma_k)$, $i = 0,1,\ldots,N_x; j = 0,1,\ldots,N_y; k = 0,1,\ldots,N_z$. The detail process and formulations can be found in our former work [17]. Especially the transformation of derivative operator to square matrix, like $\partial/\partial\alpha \Rightarrow D_\alpha$, is given in Ref. [17]. Though they were presented for one-dimensional problem, they can be extended for present three-dimensional system straight forward. The derivative operators in Eq. (5) are finally substituted by the discretized derivative matrices. Then the discretized form of Eq. (5) reads

$$\sum_l A_{i,l}I^m_{l,j,k} + \sum_l B_{j,l}I^m_{i,l,k} + \sum_l C_{k,l}I^m_{i,j,l} + K_a I^m_{i,j,l} = F_{i,j,k} \tag{8}$$

where A, B, and C are square matrices associated with differential operators in each of three dimensions, for example $A = \mu^m\left(\frac{2}{X_2-X_1}\right)D_\alpha$; I^m is the 3D solution matrix but in m direction; and F is the known right hand side term, further $F_{i,j,k} = K_a(I_b)_{i,j,k} = K_a\sigma T^4_{i,j,k}/\pi$. Please note that, Eq. (8) is a separable matrix equation, and the constant coefficient K_a can be incorporated into A, or B or C. Thus Eq. (8) can be rewritten as the following form

$$A\square_{(1)}I^m + I^m\square_{(2)}B + I^m\square_{(3)}C = F \tag{9}$$

In above equations, the matrix B is a transpose of $\eta^m\left(\frac{2}{Y_2-Y_1}\right)D_\beta$.

It should be noted that, the square matrix D_α, which involves the first derivative respect to α, is the function of grid points $\alpha_i(i = 0,1,\ldots,N_x)$ alone, and it is only needed to be computed once for all in the preparing computation. For the mth direc-

tion, the μ^m is constant, and the factor $2/(X_2 - X_1)$ is fixed, thus the matrix A is only needed to be computed once for all. Similarly, matrices B, C, and F are needed to be computed once for all in the preparing computation before the solving of matrix Eq. (9).

2.3. Boundary conditions

The matrix Eq. (9) has to be solved with appropriate boundary conditions. Unlike in CFD, the boundary conditions import is something cumbersome but not difficulty due to the direction characteristic of radiation. All boundary conditions in present work belong to Dirichlet type.

Let we go back to Eq. (8) with the coefficient K_a being incorporated into A, and assume the direction cosines (μ^m, η^m, ξ^m) of mth direction all have positive values. After the boundary conditions import, Eq. (8) becomes as another dummy summations form

$$\sum_{l=1}^{N_x} A_{i,l} I^m_{l,j,k} + \sum_{l=1}^{N_y} B_{j,l} I^m_{i,l,k} + \sum_{l=1}^{N_z} C_{k,l} I^m_{i,j,l} = F_{i,j,k} \tag{10}$$

This time the right hand side of Eq. (10) is $F_{i,j,k} = f_{i,j,k} - f^{(BC)}_{i,j,k}$, in which the boundary conditions are taken into account, and the known quantities $f^{(BC)}_{i,j,k}$ on the left-hand side of Eq. (8) were transferred to the right hand side. The detail presentation of $f^{(BC)}_{i,j,k}$, when $(\mu^m > 0, \eta^m > 0, \xi^m > 0)$ for example, is

$$f^{(BC)}_{i,j,k} = A_{i,0} I_{0,j,k} + B_{j,0} I_{i,0,k} + C_{k,0} I_{i,j,0} \tag{11}$$

The physical meaning of $f^{(BC)}_{i,j,k}$ should be clear. For $\mu^m > 0, I_{0,j,k}$ are known and will be imported as positive boundary conditions, while $I_{N_x,j,k}$ are unknowns and should be solved as negative boundary values. The situations for $\eta^m > 0$ and $\xi^m > 0$ are the similar.

For a whole 3D system, they are eight kinds of boundary conditions due to the combinations of direction cosines, they are, $(\mu^m > 0, \eta^m > 0, \xi^m > 0)$, $(\mu^m > 0, \eta^m > 0, \xi^m < 0)$, $(\mu^m > 0, \eta^m < 0, \xi^m > 0)$, $(\mu^m > 0, \eta^m < 0, \xi^m < 0)$, $(\mu^m < 0, \eta^m > 0, \xi^m > 0)$, $(\mu^m < 0, \eta^m > 0, \xi^m < 0)$, $(\mu^m < 0, \eta^m < 0, \xi^m > 0)$, $(\mu^m < 0, \eta^m < 0, \xi^m < 0)$.

It should be noticed that, when the known values $I_{i,j,k}$ are at corners or on edges of the system, their values may be related to three or two surfaces. If there exit discontinuous boundary conditions, their values will take the mathematical mean of three or two surfaces' values [11].

Finally, we get the Chebyshev matrix equations for discrete ordinates equations after boundary conditions import

$$\widetilde{A} \square_{(1)} \widetilde{I}^m + \widetilde{I}^m \square_{(2)} \widetilde{B} + \widetilde{I}^m \square_{(3)} \widetilde{C} = \widetilde{F} \tag{12}$$

where matrices $\widetilde{A}, \widetilde{B}$ and $\widetilde{C}$ are still square and related to the first derivatives with respect to three coordinates separately in Cartesian system, $\widetilde{I}^m$ is the 3D solution matrix in m direction, and $\widetilde{F}$ is the known right hand side. It is clear that the complex values are included in eigenvalues and the corresponding eigenvectors of all coefficient matrices $\widetilde{A}, \widetilde{B}$ and $\widetilde{C}$. Thus the direct and efficient matrix-diagonalization method is no longer suitable for Eq. (12).

3. Schur-decomposition for Eq. (12)

Now the task is to get the unique solutions of Eq. (12) using Schur-decomposition.

Taking any one direction m, we rewrite Eq. (12) as a general form, in which the up index m is omitted, like

$$A \square_{(1)} X + X \square_{(2)} B + X \square_{(3)} C = D \tag{13}$$

where the real matrices A, B, C and D are dimensions of $m \times m, n \times n, l \times l$ and $m \times n \times l$, respectively, the unknown matrix X is dimension of $m \times n \times l$.

Throughout the remaining part of this paper, we denote the transpose of matrix A by A^T, the quasi-upper or quasi-lower triangular form after Schur-reduction of A by A', the kth layer of 3D matrix X by $X^{(k)}$. We use the small letters to represent the entries of matrices.

3.1. The necessary and sufficient condition for the existence of unique solution to Eq. (13)

By applying Schur-decomposition, the matrices A, B and C can be reduced to triangular forms [9]

$$A' = U^T A U = \begin{pmatrix} a'_{1,1} & & & \\ a'_{2,1} & a'_{2,2} & & \\ \vdots & \vdots & \ddots & \\ a'_{m,1} & a'_{m,2} & \cdots & a'_{m,m} \end{pmatrix}, \quad B' = V^T B V = \begin{pmatrix} b'_{1,1} & b'_{1,2} & \cdots & b'_{1,n} \\ & b'_{2,2} & \cdots & b'_{2,n} \\ & & \ddots & \vdots \\ & & & b'_{n,n} \end{pmatrix}, \quad C' = W^T C W = \begin{pmatrix} c'_{1,1} & c'_{1,2} & \cdots & c'_{1,l} \\ & c'_{2,2} & \cdots & c'_{2,l} \\ & & \ddots & \vdots \\ & & & c'_{l,l} \end{pmatrix}.$$

where the matrices U, V and W are orthogonal similarity transformations [8], $a'_{i,i} \in \sigma(A), (i = 1,2,\ldots,m), b'_{j,j} \in \sigma(B)$, $(j = 1,2,\ldots,n), c'_{k,k} \in \sigma(C), (k = 1,2,\ldots,l)$. $\sigma(A)$ means the concourse of eigenvalues of matrix A.

Eq. (13) can be rewritten as the following form by replacing X with $U\square_{(1)}X'\square_{(3)}W^T\square_{(2)}V^T$ and D with $U\square_{(1)}D'\square_{(3)}W^T\square_{(2)}V^T$

$$A'\square_{(1)}X' + X'\square_{(2)}B' + X'\square_{(3)}C' = D' \tag{14}$$

where $X' = \begin{pmatrix} X'^{(l)} \\ \vdots \\ X'^{(2)} \\ X'^{(1)} \end{pmatrix}$, $D' = \begin{pmatrix} D'^{(l)} \\ \vdots \\ D'^{(2)} \\ D'^{(1)} \end{pmatrix}$, and each $X'^{(k)}$ or $D'^{(k)}$ is a $m \times n$ matrix. Regarding $c'_{k+1,k} = 0$, thus

$$\begin{cases} A'X'^{(1)} + X'^{(1)}(B' + c'_{k,k}I) = D'^{(1)}, & k = 1 \\ A'X'^{(k)} + X'^{(k)}(B' + c'_{k,k}I) = D'^{(k)} - \sum_{t=1}^{k-1} c'_{t,k}X'^{(t)}, & k = 2,3,\ldots,l \end{cases} \tag{15}$$

where I in above equation is the identity matrix.

Now the 3D matrix Eq. (14) is reduced to 2D Sylvester Eq. (15). We have known that, for the Sylvester equation, if and only if $\sigma_i(A') + \sigma_j(B' + c'_{k,k}I) \neq 0 (i = 1,2,\ldots,m; j = 1,2,\ldots,n; k = 1,2,\ldots,l)$, Eq. (15) has unique solution. While, $\sigma_i(A') + \sigma_j(B' + c'_{k,k}I) = \sigma_i(A') + \sigma_j(B') + \sigma_k(c'_{k,k}I)$ and $\sigma_k(c'_{k,k}I) = \sigma_k(C') = \sigma_k(C), \sigma_i(A') = \sigma_i(A), \sigma_j(B') = \sigma_j(B)$, therefore, for Eqs. (13) or (14), the necessary and sufficient condition for the existence of unique solution is $\sigma_i(A) + \sigma_j(B) + \sigma_k(C) \neq 0 (i = 1,2,\ldots,m; j = 1,2,\ldots,n; k = 1,2,\ldots,l)$. Please note that this condition is suitable for Eq. (13) whether $\sigma_i(A), \sigma_j(B)$ and $\sigma_k(C)$ are real or complex.

3.2. Solving process

The matrix A is reduced to real, block quasi-lower triangular form (real Schur form) A' by an orthogonal similarity transformation U.

$$A' = U^TAU = \begin{pmatrix} A'_{1,1} & & & \\ A'_{2,1} & A'_{2,2} & & \\ \vdots & \vdots & \ddots & \\ A'_{p,1} & A'_{p,2} & \cdots & A'_{p,p} \end{pmatrix}$$

where each block $A'_{i,i} (i = 1,2,\ldots,p)$ is of order at most two (if A does not have any complex eigenvalue, A' will be a triangular matrix). Similarly, B and C are reduced to quasi-upper triangular forms, respectively.

$$B' = V^TBV = \begin{pmatrix} B'_{1,1} & B'_{1,2} & \cdots & B'_{1,q} \\ & B'_{2,2} & \cdots & B'_{2,q} \\ & & \ddots & \vdots \\ & & & B'_{q,q} \end{pmatrix}$$

$$C' = W^TCW = \begin{pmatrix} C'_{1,1} & C'_{1,2} & \cdots & C'_{1,r} \\ & C'_{2,2} & \cdots & C'_{2,r} \\ & & \ddots & \vdots \\ & & & C'_{r,r} \end{pmatrix}$$

where again each $B'_{j,j} (j = 1,2,\ldots,q)$, and $C'_{k,k} (k = 1,2,\ldots,r)$ is of order at most two. In above transformations, matrices U, V and W are real unitary matrices and dimensions of $m \times m, n \times n$ and $l \times l$, respectively. They are guaranteed by Schur's triangularization theorem. If

$$D' = U^T\square_{(1)}D\square_{(3)}W\square_{(2)}V$$

and

$$X' = U^T\square_{(1)}X\square_{(3)}W\square_{(2)}V$$

then Eq. (13) is equal to

$$A'\square_{(1)}X' + X'\square_{(2)}B' + X'\square_{(3)}C' = D' \tag{16}$$

Please note that, the presentations of matrices A', B' and C' in Eq. (16) are different from those in Eq. (14). Now the unknown solution matrix is X'. The solving procedure of Eq. (16) will be switched ceaselessly according to the situations of different eigenvalues of C.

3.2.1. Switch one: for the real eigenvalues of C

Under this situation, $c'_{k+1,k}$ is zero, Eq. (16) can be reduced to the form of Eq. (15).

Set $F'^{(k)} = D'^{(k)} - \sum_{t=1}^{k-1} c'_{t,k} X'^{(t)}$, now Eq. (16) is reduced to the 2D matrix equation.

$$A'X'^{(k)} + X'^{(k)}(B' + c'_{k,k}I) = F'^{(k)} \tag{17}$$

where $X'^{(k)} = \begin{pmatrix} x_1'^{(k)} \\ x_2'^{(k)} \\ \vdots \\ x_m'^{(k)} \end{pmatrix}$ and $F'^{(k)} = \begin{pmatrix} f_1'^{(k)} \\ f_2'^{(k)} \\ \vdots \\ f_m'^{(k)} \end{pmatrix}$. The solving of Eq. (17) will be switched ceaselessly using a sub switch according to the eigenvalues of A, say, whether they are real or complex.

Case 1: the eigenvalues of A are real Under this case, $a'_{i,i+1}$ is zero, $x_i'^{(k)}$ can be determined by solving the lower triangular matrix system.

$$x_i'^{(k)}\left[B' + \left(a'_{i,i} + c'_{k,k}\right)I\right] = f_i'^{(k)} - \sum_{t=1}^{i-1} a'_{i,t} x_t'^{(k)} \tag{18}$$

Case 2: the eigenvalues of A are complex Under this case, the complex values which appear in eigenvalues of A are conjugate. If $a'_{i,i+1}$ is nonzero, by combining rows i and $i+1$ in Eq. (17), we find

$$\begin{pmatrix} a'_{i,i} & a'_{i,i+1} \\ a'_{i+1,i} & a'_{i+1,i+1} \end{pmatrix} \times \begin{pmatrix} x_i'^{(k)} \\ x_{i+1}'^{(k)} \end{pmatrix} + \begin{pmatrix} x_i'^{(k)} \\ x_{i+1}'^{(k)} \end{pmatrix} \times (B' + c'_{k,k}I) = \begin{pmatrix} f_i'^{(k)} \\ f_{i+1}'^{(k)} \end{pmatrix} - \begin{pmatrix} a'_{i,1} & \cdots & a'_{i,i-1} & 0 & \cdots & 0 \\ a'_{i+1,1} & \cdots & a'_{i+1,i-1} & 0 & \cdots & 0 \end{pmatrix} \times \begin{pmatrix} x_1'^{(k)} \\ x_2'^{(k)} \\ \vdots \\ x_m'^{(k)} \end{pmatrix} \tag{19}$$

Because the complex eigenvalues of A are conjugate, therefore $a'_{i,i} = a'_{i+1,i+1}$, thus Eq. (19) can be simplified as

$$\begin{cases} a'_{i,i+1} x_{i+1}'^{(k)} + x_i'^{(k)}\left[B' + \left(a'_{i,i} + c'_{k,k}\right)I\right] = f_i'^{(k)} - \sum_{t=1}^{i-1} a'_{i,t} x_t'^{(k)} \\ a'_{i+1,i} x_i'^{(k)} + x_{i+1}'^{(k)}\left[B' + \left(a'_{i,i} + c'_{k,k}\right)I\right] = f_{i+1}'^{(k)} - \sum_{t=1}^{i-1} a'_{i+1,t} x_t'^{(k)} \end{cases} \tag{20}$$

This is a linear system for $x_i'^{(k)}$ and $x_{i+1}'^{(k)}$. Eqs. (18) or (20) can be solved successively for $x_1'^{(k)}, x_2'^{(k)}, \ldots, x_m'^{(k)}$, and further for $X'^{(k)}$.

3.2.2. Switch two: for the complex eigenvalues of C

Under this situation, $c'_{k+1,k}$ is assumed to be nonzero. Eq. (16) can be rewritten as the elements summation form

$$\sum_{t=1}^{m} a'_{i,t} x'_{t,j,k} + \sum_{t=1}^{n} b'_{t,j} x'_{i,t,k} + \sum_{t=1}^{l} x'_{i,j,t} c'_{t,k} = d'_{i,j,k} \tag{21}$$

and the matrix form in two-dimensional of Eq. (21) reads

$$A'X'^{(k)} + X'^{(k)}B' + \sum_{t=1}^{l} c_{t,k} X'^{(t)} = D'^{(k)}, \quad k = 1, 2, \ldots l \tag{22}$$

Eq. (22) can be reduced to

$$\begin{cases} A'X'^{(k)} + X'^{(k)}B' + \sum_{t=1}^{k+1} c_{t,k} X'^{(t)} = D'^{(k)} \\ A'X'^{(k+1)} + X'^{(k+1)}B' + \sum_{t=1}^{k+1} c_{t,k+1} X'^{(t)} = D'^{(k+1)} \end{cases} \tag{23}$$

Rearranging Eq. (23), one gets the final form

$$\begin{cases} A'X'^{(k)} + X'^{(k)}\left(B' + c'_{k,k}I\right) + c'_{k+1,k} X'^{(k+1)} = D'^{(k)} - \sum_{t=1}^{k-1} c'_{t,k} X'^{(t)} \\ c'_{k,k+1} X'^{(k)} + A'X'^{(k+1)} + X'^{(k+1)}\left(B' + c'_{k+1,k+1}I\right) = D'^{(k+1)} - \sum_{t=1}^{k-1} c'_{t,k+1} X'^{(t)} \end{cases} \tag{24}$$

In above equation, the first two unknown matrices $X'^{(1)}$ and $X'^{(2)}$ can be solved directly because the right hand sides are known values of $D'^{(1)}$ and $D'^{(2)}$ when $k=1$. After the solving of $X'^{(1)}$ and $X'^{(2)}$, the right hand sides of Eq. (24) can be determined recurrently from $F'^{(k)} = D'^{(k)} - \sum_{t=1}^{k-1} c'_{t,k} X'^{(t)}$ and $F'^{(k+1)} = D'^{(k+1)} - \sum_{t=1}^{k-1} c'_{t,k+1} X'^{(t)}$. In other words, when $X'^{(1)}$ and $X'^{(2)}(k=1)$ are known, $F'^{(3)}$ and $F'^{(4)}$ can be computed, then $X'^{(3)}$ and $X'^{(4)}(k=3)$ can be solved from Eq. (24), and so on.

Again, the solving of Eq. (24) will be switched ceaselessly according to the eigenvalues of A, say, whether they are real or complex.

Case 1: the eigenvalues of A are real Under this case, $a'_{i,i+1}$ is zero, then Eq. (24) can be simplified as

$$\begin{cases} x_i'^{(k)}\left[B' + \left(a'_{i,i} + c'_{k,k}\right)I\right] + c'_{k+1,k} x_i'^{(k+1)} = f_i'^{(k)} - \sum_{t=1}^{i-1} a'_{i,t} x_t'^{(k)} \\ x_i'^{(k+1)}\left[B' + \left(a'_{i,i} + c'_{k+1,k+1}\right)I\right] + c'_{k,k+1} x_i'^{(k)} = f_i'^{(k+1)} - \sum_{t=1}^{i-1} a'_{i,t} x_t'^{(k+1)} \end{cases} \tag{25}$$

Case 2: the eigenvalues of A are complex Under this case, the complex values which appear in eigenvalues of A are conjugate. If $a'_{i,i+1}$ is nonzero, Eq. (24) are a group like

$$\begin{cases} \sum_{t=1}^{m} a'_{i,t} x_t'^{(k)} + x_i'^{(k)}\left(B' + c'_{k,k} I\right) + c'_{k+1,k} x_i'^{(k+1)} = f_i'^{(k)}, \\ \sum_{t=1}^{m} a'_{i,t} x_t'^{(k+1)} + x_i'^{(k+1)}\left(B' + c'_{k+1,k+1} I\right) + c'_{k,k+1} x_i'^{(k)} = f_i'^{(k+1)}, \end{cases} \quad i = 1, 2, \ldots, m \tag{26}$$

By combining rows i and $i+1$ in Eq. (26), we find

$$\begin{cases} \sum_{t=1}^{i+1} a'_{i,t} x_t'^{(k)} + x_i'^{(k)}\left(B' + c'_{k,k} I\right) + c'_{k+1,k} x_i'^{(k+1)} = f_i'^{(k)} \\ \sum_{t=1}^{i+1} a'_{i+1,t} x_t'^{(k)} + x_{i+1}'^{(k)}\left(B' + c'_{k,k} I\right) + c'_{k+1,k} x_{i+1}'^{(k+1)} = f_{i+1}'^{(k)} \\ \sum_{t=1}^{i+1} a'_{i,t} x_t'^{(k+1)} + x_i'^{(k+1)}\left(B' + c'_{k+1,k+1} I\right) + c'_{k,k+1} x_i'^{(k)} = f_i'^{(k+1)} \\ \sum_{t=1}^{i+1} a'_{i+1,t} x_t'^{(k+1)} + x_{i+1}'^{(k+1)}\left(B' + c'_{k+1,k+1} I\right) + c'_{k,k+1} x_{i+1}'^{(k)} = f_{i+1}'^{(k+1)} \end{cases} \tag{27}$$

Rearranging Eq. (27), one gets the final form

$$\begin{cases} x_i'^{(k)}\left[B' + \left(a'_{i,i} + c'_{k,k}\right)I\right] + a'_{i,i+1} x_{i+1}'^{(k)} + c'_{k+1,k} x_i'^{(k+1)} = f_i'^{(k)} - \sum_{t=1}^{i-1} a'_{i,t} x_t'^{(k)} \\ a'_{i+1,i} x_i'^{(k)} + x_{i+1}'^{(k)}\left[B' + \left(a'_{i+1,i+1} + c'_{k,k}\right)I\right] + c'_{k+1,k} x_{i+1}'^{(k+1)} = f_{i+1}'^{(k)} - \sum_{t=1}^{i-1} a'_{i+1,t} x_t'^{(k)} \\ x_i'^{(k+1)}\left[B' + \left(a'_{i,i} + c'_{k+1,k+1}\right)I\right] + a'_{i,i+1} x_{i+1}'^{(k+1)} + c'_{k,k+1} x_i'^{(k)} = f_i'^{(k+1)} - \sum_{t=1}^{i-1} a'_{i,t} x_t'^{(k+1)} \\ a'_{i+1,i} x_i'^{(k+1)} + x_{i+1}'^{(k+1)}\left[B' + \left(a'_{i+1,i+1} + c'_{k+1,k+1}\right)I\right] + c'_{k,k+1} x_{i+1}'^{(k)} = f_{i+1}'^{(k+1)} - \sum_{t=1}^{i-1} a'_{i+1,t} x_t'^{(k+1)} \end{cases} \tag{28}$$

Again, Eqs. (25) or (28) can be solved successively for $x_1'^{(k)}, x_2'^{(k)}, \ldots, x_m'^{(k)}$, and further for $X'^{(k)}$.

Whether for switch one or switch two, after all $X'^{(1)}, X'^{(2)}, \ldots, X'^{(l)}$ being ready, the solution matrix X in Eq. (13) can be computed through $X = U\square_{(1)} X \square_{(3)} W^T \square_{(2)} V^T$.From above process, we can evaluate the operations. In fact, the solving Eq. (13) is of l times 2D Sylvester equation solution. For 2D Sylvester equation solution by Schur-decomposition, the operations can be found in recent reference [25] and take the value of $(4+8\omega)(m^3+n^3)+5mn(m+n)$, where ω is the average number of QR algorithm. Therefore, it is not difficult to know that, for Eq. (13), the operations take the value of $(4+8\omega)(m^3+n^3+l^3)+[5mn(m+n)]l$.

4. Numerical results and discussion

In principal, the 3D matrix Eq. (13) can be reduced to 2D one (Sylvester equation) using tensor product technique [11,26] like

$$AX + XC = D \tag{29}$$

where this time the matrix A is a tensor product of original matrices A and B in Eq. (13), and the resolution matrix X and the known right hand side matrix D are transformed to 2D ones correspondingly. After that, the direct Schur-decomposition method for 2D matrix equation is adopted to solve our problem successfully. However, as mentioned in Refs. [11,26], the computer memory requirement is too heavy for some even moderate accuracy computations due to tensor product, special for large resolutions needing cases. For example, if the original square matrices A and B are dimensions of $m \times m$ and $n \times n$ separately, the resultant matrix after tensor product will be dimension of $(m \times n) \times (m \times n)$. Due to the large memory needing, the CPU time increases exponentially.

Certainly, there are also many other methods which are available for the present physical problem. For example, in very recent, the efforts to enhance the stabilities and to fast the speeds of the solutions of DOM equations [27–29] were made. However, according to the authors' knowledge, there are not any direct solution algorithms for DOM equations. In order to give detail comparisons and show the superiorities of the Schur-decomposition for 3D matrix equations, the authors developed three methods.

The first one is the standard DOM [22,24,30,31] in which the iterative solution process is needed. In DOM, the same weighted diamond-difference scheme which relates the cell edge radiant intensities to the cell center radiant intensity is used, and the iteration was ended when a convergence criterion of $|I_p^m - I_p^{m*}|/I_p^{m*} \leqslant 10^{-8}$ was satisfied, where the I_p^m and I_p^{m*} represent previous iteration intensity values in any direction m at the center location p of any control volume and its present one, respectively.

The second one and the third one are all based on Chebyshev collocation spectral method for the discrete ordinates Eq. (2). The difference between the second and the third ones exists: in the second method, for the resultant 3D matrix Eq. (12), the Schur-decomposition is used to solve the 2D Sylvester type matrix equations after the transformation of 3D matrix equations to 2D ones by tensor product; while in the third method, the Schur-decomposition, which is developed by authors, is used to solve the 3D matrix Eq. (12) directly. Please remember that the second and the third methods can provide exactly the same results under the same inputs.

For all above three methods, an angular quadrature of SSD_{2a} with 48 directions in whole 4π solid angle [31] is adopted for the angular discritization, and the codes are designed using both MATLAB and FORTRAN 95 computer languages. The comparisons are made on a personal computer with Intel(R) Core(TM)2 Duo CPU E4500 (2.20 GHz) and 2.0 GB (DDR2) memory.

4.1. Accuracy validation

To illustrate the accuracy of the direct spectral method (abbreviate to SP later) for 3D system, some typical computational results from SP are compared with those from standard DOM under the same quadrature scheme and grid points. Our DOM code was validated before in Ref. [31].

4.1.1. Radiative heat flux on the side wall

First the dimensionless heat flux densities on side wall along different lines are presented in Figs. 1–6 for different resolutions. We choose the first line which is mostly close to the center of the side wall, and the second line which is mostly close to the corner.

For the resolutions of $N_x \times N_y \times N_z = 5 \times 5 \times 21$, the results are comparatively given in Fig. 1 along the line of $(X = 0.3090, Y = 1, Z)$ and in Fig. 2 along the line of $(X = 0.8090, Y = 1, Z)$, respectively. In Fig. 1, the biggest relative error of SP with respect to DOM is 3.5877%, while in Fig. 2, its 8.4351%. Increase the resolutions up to $9 \times 9 \times 33$, the results are given along the line of $(X = 0.1736, Y = 1, Z)$ in Fig. 3 and along the line of $(X = 0.9397, Y = 1, Z)$ in Fig. 4, respectively. Now the biggest relative errors reduced to 3.2082% in Fig. 3 and 0.9734% in Fig. 4, separately. Further increase the resolutions

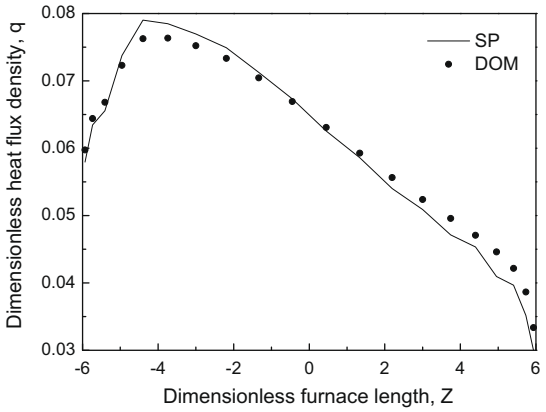

Fig. 1. Comparison of dimensionless heat flux density to the side wall along the line of $(X = 0.3090, Y = 1, Z)$ with the resolutions of $5 \times 5 \times 21$.

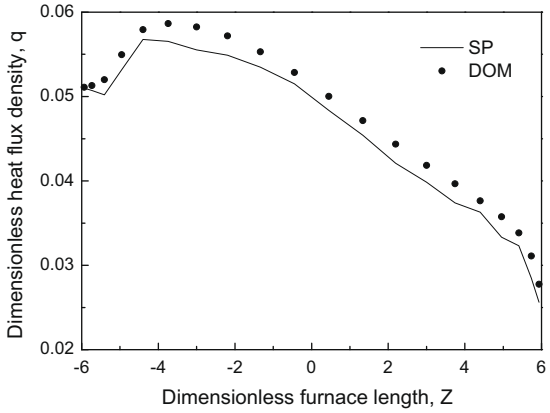

Fig. 2. Comparison of dimensionless heat flux density to the side wall along the line of $(X = 0.8090, Y = 1, Z)$ with the resolutions of $5 \times 5 \times 21$.

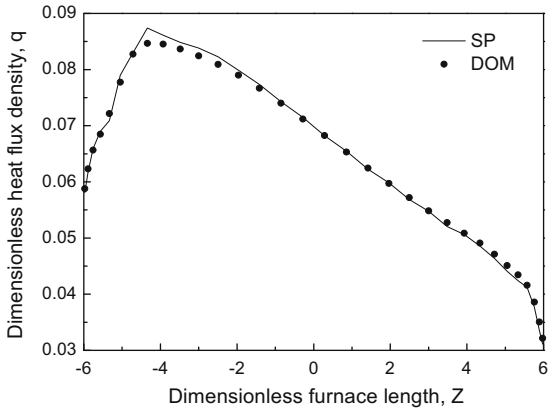

Fig. 3. Comparison of dimensionless heat flux density to the side wall along the line of $(X = 0.1736, Y = 1, Z)$ with the resolutions of $9 \times 9 \times 33$.

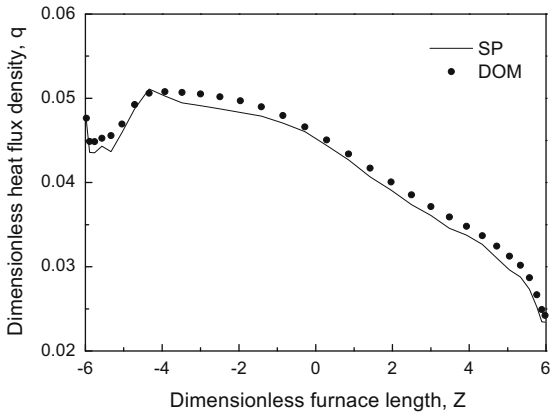

Fig. 4. Comparison of dimensionless heat flux density to the side wall along the line of $(X = 0.9397, Y = 1, Z)$ with the resolutions of $9 \times 9 \times 33$.

up to $13 \times 13 \times 45$, the results are given along the line of $(X = 0.0349, Y = 1, Z)$ in Fig. 5 and along the line of $(X = 0.9976, Y = 1, Z)$ in Fig. 6, respectively. This time the biggest relative errors are 2.0706% in Fig. 5 and 2.8575% in Fig. 6, separately. The computational results indicated that the biggest relative errors will not decrease obviously when the resolutions were increased more than $13 \times 13 \times 45$.

The results of dimensionless heat flux densities on the side wall show a very good agreement between the SP and the DOM.

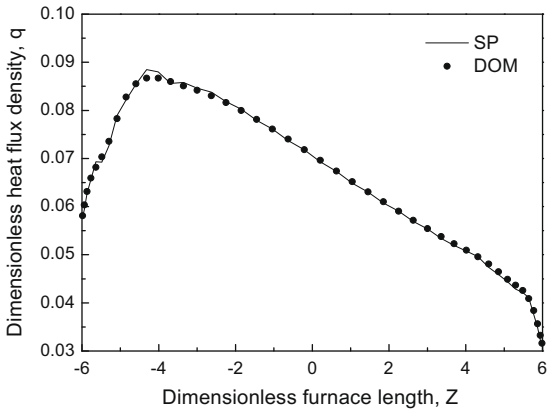

Fig. 5. Comparison of dimensionless heat flux density to the side wall along the line of $(X = 0.0349, Y = 1, Z)$ with the resolutions of $13 \times 13 \times 45$.

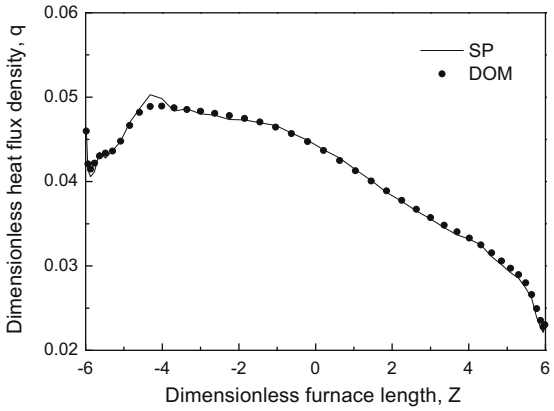

Fig. 6. Comparison of dimensionless heat flux density to the side wall along the line of $(X = 0.9976, Y = 1, Z)$ with the resolutions of $13 \times 13 \times 45$.

4.1.2. Point values of radiative source term

Second the dimensionless radiative source terms along different lines are presented in Figs. 7–15 for different resolutions. We choose the first line which is mostly close to the center of the furnace, the second line which is mostly close to the side wall, the third line which is mostly close to the corner.

For the resolutions of $5 \times 5 \times 21$, the results are comparatively given in Figs. 7–9 along the lines of $(X = 0.3090, Y = 0.3090, Z)$, $(X = 0.3090, Y = 0.8090, Z)$, and $(X = 0.8090, Y = 0.8090, Z)$, respectively. The biggest relative errors of SP with respect to DOM are 5.7233%, 1.3594%, and 0.8759%, separately. Increase the resolutions up to $9 \times 9 \times 33$, the results are given in Figs. 10–12 along the lines of $(X = 0.1736, Y = 0.1736, Z)$, $(X = 0.1736, Y = 0.9397, Z)$, and $(X = 0.9397, Y = 0.9397, Z)$, respectively. Then the biggest relative errors reduced to 4.7741%, 1.6056%, and 0.8001%, separately. Further increase the resolutions up to $13 \times 13 \times 45$, the results are given in Figs. 13–15 along the lines of $(X = 0.0349, Y = 0.0349, Z)$, $(X = 0.0349, Y = 0.9976, Z)$, and $(X = 0.9976, Y = 0.9976, Z)$, respectively. This time the biggest relative errors reduced to 2.3377%, 1.4810%, and 0.4182%, separately.

Again, the results of dimensionless source terms within the furnace show a very good agreement between the SP and the DOM.

4.2. CPU time comparison with standard DOM

The most attractive advantage of direct spectral method over the standard DOM is its high speed. However, even though the SP with 2D Schur-decomposition and the SP with 3D Schur-decomposition solvers are all direct, their CPU time costs can be very different. The CPU time cost comparisons are listed in Tables 2 and 3 when the MATLAB and FORTRAN 95 computer languages are used for the codes design, respectively. The CPU times of three methods, which are developed in present work, are listed against the resolutions.

From Table 2, when the resolutions increase from $N_x \times N_y \times N_z = 5 \times 5 \times 21$ up to $N_x \times N_y \times N_z = 17 \times 17 \times 57$, the CPU time increase from 0.4617 up to 7.6003 seconds for SP with 3D Schur-decomposition, from 0.3156 up to 133.0637 seconds for SP with 2D Schur-decomposition, but from 2.5385 up to 543.6464 seconds for standard DOM. That means, for the ade-

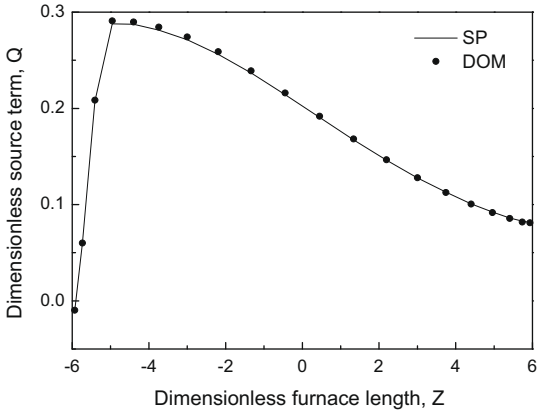

Fig. 7. Comparison of dimensionless source term alone the line of $(X = 0.3090, Y = 0.3090, Z)$ with the resolutions of $5 \times 5 \times 21$.

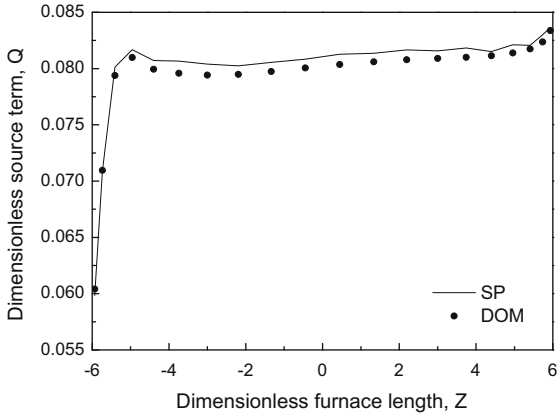

Fig. 8. Comparison of dimensionless source term alone the line of $(X = 0.3090, Y = 0.8090, Z)$ with the resolutions of $5 \times 5 \times 21$.

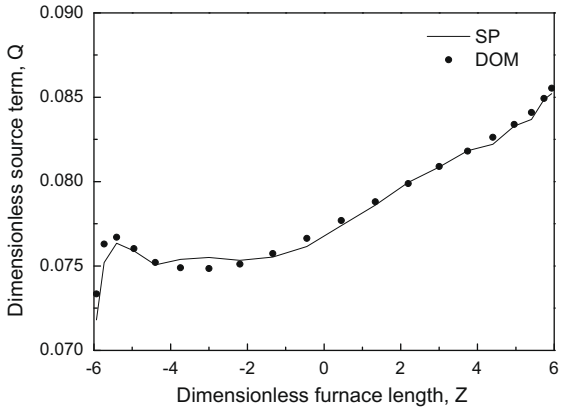

Fig. 9. Comparison of dimensionless source term alone the line of $(X = 0.8090, Y = 0.8090, Z)$ with the resolutions of $5 \times 5 \times 21$.

quate accuracy requirements, $N_x \times N_y \times N_z = 13 \times 13 \times 45$ for example, almost one tenth CPU time is needed when SP with 3D Schur-decomposition solver is used compared SP with 2D Schur-decomposition solver, and almost one fiftieth CPU time is needed compared with the standard DOM.

It is well known that the MATLAB is the most suitable computer language for matrix operations. While, most of computations in the standard DOM are not relative to matrix operations. Thereby the FORTRAN 95 computer language is used to

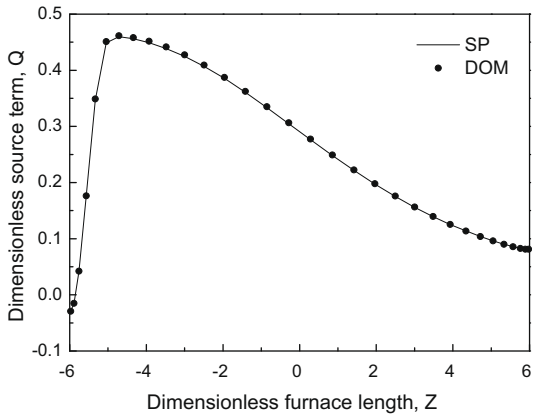

Fig. 10. Comparison of dimensionless source term alone the line of $(X = 0.1736, Y = 0.1736, Z)$ with the resolutions of $9 \times 9 \times 33$.

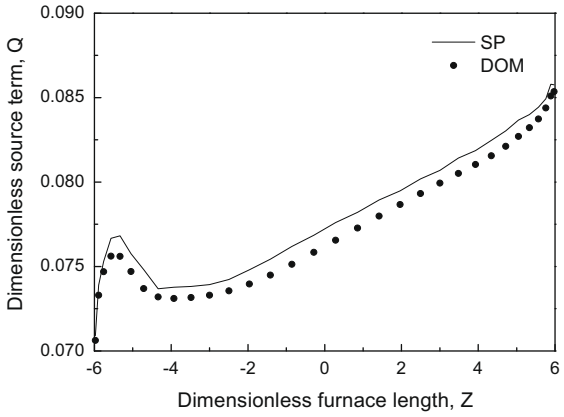

Fig. 11. Comparison of dimensionless source term alone the line of $(X = 0.1736, Y = 0.9397, Z)$ with the resolutions of $9 \times 9 \times 33$.

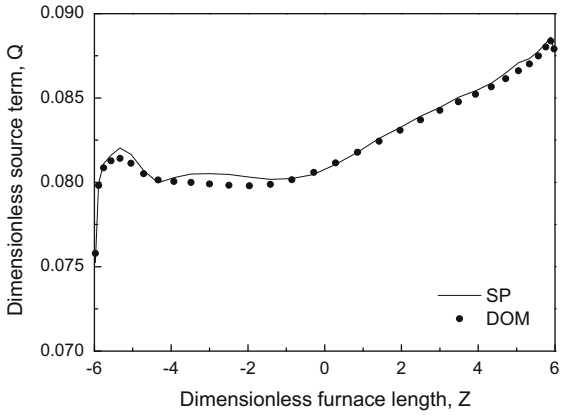

Fig. 12. Comparison of dimensionless source term alone the line of $(X = 0.9397, Y = 0.9397, Z)$ with the resolutions of $9 \times 9 \times 33$.

design three codes for three methods accordingly. The results listed in Table 3 show that, the CPU time costs of SP with 3D Schur-decomposition are still the least for an adequate accuracy requirement, and those of SP with 2D Schur-decomposition are the most. When the resolutions reach $N_x \times N_y \times N_z = 17 \times 17 \times 57$, the memory is overflow for SP with 2D Schur-decomposition due to tensor product.

Please note that, the present computational results cannot be compared with the exact solutions which are listed in Ref. [20] due the intrinsic characteristics of collocation points of Chebyshev collocation spectral method, in other words, the grid

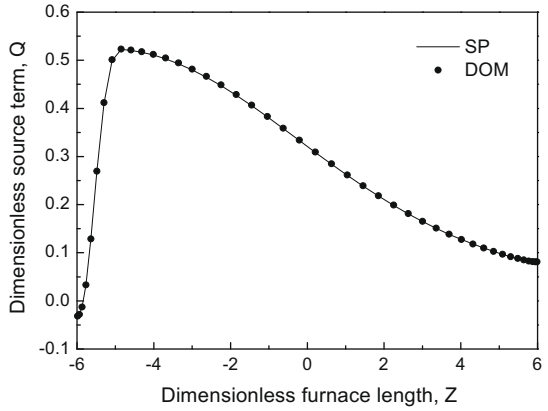

Fig. 13. Comparison of dimensionless source term alone the line of $(X = 0.0349, Y = 0.0349, Z)$ with the resolutions of $13 \times 13 \times 45$.

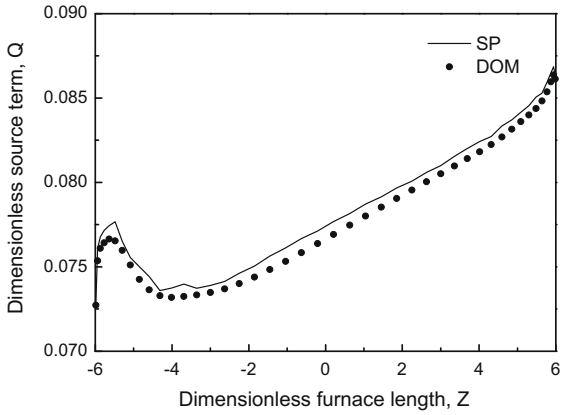

Fig. 14. Comparison of dimensionless source term alone the line of $(X = 0.0349, Y = 0.9976, Z)$ with the resolutions of $13 \times 13 \times 45$.

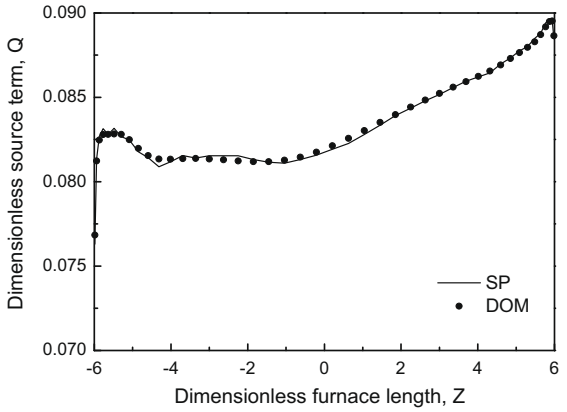

Fig. 15. Comparison of dimensionless source term alone the line of $(X = 0.9976, Y = 0.9976, Z)$ with the resolutions of $13 \times 13 \times 45$.

points cannot be taken exactly the same on which the exact solutions exit. Therefore, the comparisons of dimensional radiative heat flux and source term in this section could not verify the accuracy of the present method, because the standard DOM is also an approximated method. The given relative errors of SP with respect to standard DOM just illustrate that, both SP and DOM consist with each other and provide the good accurate results with the increasing of resolutions.

Table 2
CPU time comparisons between the standard DOM and SP using MATLAB computer language.

Resolutions ($N_x \times N_y \times N_z$)	CPU time (second)		
	SP with 2D Schur-decomposition	SP with 3D Schur-decomposition	Standard DOM
$5 \times 5 \times 21$	0.3156	0.4614	2.5385
$9 \times 9 \times 33$	2.7485	1.4234	25.4818
$13 \times 13 \times 45$	22.8985	3.5341	183.9122
$17 \times 17 \times 57$	133.0637	7.6003	543.6464

Table 3
CPU time comparisons between the standard DOM and SP using FORTRAN 95 computer language.

Resolutions ($N_x \times N_y \times N_z$)	CPU time (second)		
	SP with 2D Schur-decomposition	SP with 3D Schur-decomposition	Standard DOM
$5 \times 5 \times 21$	2.8758	0.7196	2.0473
$9 \times 9 \times 33$	48.2664	2.2157	16.7975
$13 \times 13 \times 45$	725.4545	6.6865	169.7954
$17 \times 17 \times 57$	Stack Overflow	17.6245	502.5462

5. Conclusions and remarks

After the angular discretization by DOM, the three-dimensional radiative discrete ordinates equations are discretized by Chebyshev collocation spectral method in space. The resultant 3D matrix equations cannot be solved by matrix-diagonalization directly and efficiently because the eigen-system is complex rather than real. Then the Schur-decomposition, which is special efficient and suitable for complex eigen-systems, for 3D matrix equations is developed to avoid the complex number computations, and is used to directly solve the radiative matrix equations successfully.

In order to verify the outstanding superiorities of the Schur-decomposition for 3D radiative matrix equations, three codes for standard DOM, SP with 2D Schur-decomposition and SP with 3D Schur-decomposition are designed using MATLAB and FORTRAN 95 computer language, respectively. In SP with 2D Schur-decomposition, the 3D radiative matrix equations are transformed to 2D ones by tensor product. A typical case of radiative heat transfer within a rectangular furnace, in which there are absorbing-emitting, and radiative gray media, is adopted to make comparisons. The results show that, the present SP with 2D or 3D Schur-decomposition methods can provide good accuracy, especially, the CPU time costs of the SP with 3D Schur-decomposition method are almost one thirtieth to one fiftieth of the standard DOM under the same computer inputs.

In present, the physical model, which was adopted from reference, is relatively simple. For example, the participating medium is absorbing-emitting, but no-scattering, radiative gray; and the boundaries are just black. In Refs. [16,17], the effect of angular quadrature on the computational accuracy are investigated for 1D problems, but in 3D systems, it should be investigated more detailedly. While, those will be our future works.

Acknowledgment and announcement

This work was supported by the National Fundamental Research Programme of China (No. 2006CB601203). The corresponding author applied the project of "the Spectral methods for Thermal Radiation" from the National Nature Science Foundation of China three times, but all with rejections.

References

[1] G.H. Golub, S. Nash, C.F. Van Loan, A Hesenberg–Schur method for the problem $AX + XB = C$, IEEE Trans. Auto. Control 24 (1979) 909–913.
[2] S.D. Brierly, E.B. Lee, Solution of the equation $A(z)X(z) - X(z)B(z) = C(z)$ and its application to the stability of generalized linear system, Int. J. Control 40 (1984) 1065–1075.
[3] R.E. Lynch, J.R. Rice, D.H. Thomas, Direct solution of partial differential equations by tensor product method, Numer. Math. 6 (1964) 185–199.
[4] D.B. Haidvogel, T.A. Zang, The accurate solution of Poisson's equation by expansion in Chebyshev polynomials, J. Comput. Phys. 30 (1979) 167–180.
[5] P. Haldenwang, G. Labrosse, S. Abboude, M.O. Deville, Chebyshev 3-D spectral and 2-D pseudospectral solvers for the Helmholtz equation, J. Comput. Phys. 55 (1984) 115–128.
[6] U. Ehrenstein, R. Peyret, A Chebyshev collocation method for the Navier–Stokes equations with application to double-diffusive convection, Int. J. Numer. Methods Fluids 9 (1989) 427–452.
[7] H.-L. Chen, Y.-H. Su, B.D. Shizgal, A direct spectral collocation Poisson solver in polar and cylindrical coordinates, J. Comput. Phys. 160 (2000) 453–469.
[8] R.H. Bartels, G.W. Stewart, Solution of the matrix equation $AX + XB = C$, Commun. ACM 15 (1972) 820–826.
[9] R.A. Horn, C.R. Johnson, Topics in Matrix Analysis, Cambridge University Press, Cambridge, 1991.
[10] W.D. Hoskins, D.S. Meek, D.J. Walton, The numerical solution of the matrix equation $XA + AY = F$, BIT Numer. Math. 17 (1977) 184–190.
[11] R. Peyret, Spectral methods for incompressible viscous flow, Springer-Verlage, New York, 2002.
[12] R. Siegel, J.R. Howell, Thermal Radiation Heat Transfer, 4th ed., Taylor and Francis, Washington, DC.
[13] D. Gottlieb, S.A. Orszag, Numerical analysis of spectral methods: Theory and applications, Regional Conference Series in Applied Mathematics, vol. 28, Philadelphia, SIAM, 1977.
[14] C. Canuto, M.Y. Hussaini, A. Quarteroni, T.A. Zang, Spectral Methods in Fluid Dynamics, Springer-Verlag, Berlin, 1989.

[15] B.-W. Li, Y.-S. Sun, Y. Yu, Iterative and direct Chebyshev collocation spectral methods for one-dimensional radiative heat transfer, Int. J. Heat Mass Transfer 51 (2008) 5887–5894.
[16] Y.-S. Sun, B.-W. Li, Chebyshev collocation spectral method for one-dimensional radiative heat transfer in graded index media, Int. J. Thermal Sci. 48 (2009) 691–698.
[17] B.-W. Li, Y.-S. Sun, D.-W. Zhang, Chebyshev collocation spectral methods for coupled radiation and conduction in a concentric spherical participating medium, J. Heat Transfer 131 (2009) 062701–062709.
[18] Y.-S. Sun, B.-W. Li, Chebyshev collocation spectral approach for combined radiative and conduction heat transfer in one-dimensional semitransparent medium with graded index, Int. J. Heat Mass Transfer (2009), doi:10.1115/1.4000444.
[19] Y.-S. Sun, B.-W. Li, Spectral collocation method for transient combined radiation and conduction in an anisotropic scattering slab with graded index, J. Heat Transfer, in press.
[20] N. Selcuk, Exact solutions for radiative heat transfer in box-shaped furnaces, J. Heat Transfer 107 (1985) 648–655.
[21] B.G. Carlson, K.D. Lathrop, Computing Methods in Reactor Physics, in: H. Greenspan, C.N. Kelber, D. Okrent (Eds.), Gordon and Breach, New York, 1968.
[22] W.A. Fiveland, Discrete-ordinates solutions of the radiative transport equation for rectangular enclosures, J. Heat Transfer 106 (1984) 699–706.
[23] J.S. Truelove, Discrete-ordinates solutions of radiation transport equation, J. Heat Transfer 109 (1987) 1048–1051.
[24] J.S. Truelove, Three-dimensional radiation in absorbing-emitting-scattering media using the discrete-ordinates approximation, JQSRT 39 (1988) 27–31.
[25] C. Canuto, M.Y. Hussaini, A. Quarteroni, T.A. Zang, Spectral Methods/Fundamentals in Single Domains, Springer-Verlag, Berlin, 2006.
[26] L.N. Trefethen, Spectral Methods in MATLAB, SIAM, Oxford University, 2000.
[27] P. Henshall, P. Palmer, A leapfrog algorithm for coupled conductive and radiative transient heat transfer in participating media, Int. J. Thermal Sci. 47 (2008) 388–398.
[28] N. Selcuk, N. Doner, A 3-D radiation model for non-grey gases, JQSRT 110 (2009) 184–191.
[29] P. Edström, Numerical performance of stability enhancing and speed increasing steps in radiative transfer solution methods, J. Comput. Appl. Math. 228 (2009) 104–114.
[30] N. Selcuk, N. Kayakol, Evaluation of discrete ordinates method for radiative transfer in rectangular furnaces, Int. J. Heat Mass Transfer 40 (1997) 213–222.
[31] B.-W. Li, H.-G. Chen, J.-H. Zhou, X.-Y. Cao, K.-F. Cen, The spherical surface symmetrical equal dividing angular quadrature scheme for discrete ordinates method, J. Heat Transfer 124 (2002) 482–489.